Batch-mode mixing on centrifugal microfluidic platforms

M. Grumann, A. Geipel, L. Riegger, R. Zengerle and J. Ducrée

Received 3rd February 2005, Accepted 16th March 2005
First published as an Advance Article on the web 7th April 2005
DOI: 10.1039/b418253g

We present two novel fluidic concepts to drastically accelerate the process of mixing in batch-mode (stopped-flow) on centrifugal microfluidic platforms. The core of our simple and robust setup exhibits a microstructured disk with a round mixing chamber rotating on a macroscopic drive unit. In the first approach, magnetic beads which are prefilled into the mixing chamber are periodically deflected by a set of permanent magnets equidistantly aligned at spatially fixed positions in the lab-frame. Their radial positions alternatingly deviate by a slight positive and negative offset from the mean orbit of the chamber to periodically deflect the beads inbound and outbound during rotation. Advection is induced by the relative motion of the beads with respect to the liquid which results from the magnetic and centrifugal forces, as well as inertia. In a second approach—without magnetic beads—the disk is spun upon periodic changes in the sense of rotation. This way, inertia effects induce stirring of the liquids. As a result, both strategies accelerate mixing from about 7 minutes for mere diffusion to less than five seconds. Combining both effects, an ultimate mixing time of less than one second could be achieved.

1 Introduction

Microfluidic technologies play a key role for enabling many novel applications in the life sciences.[1–3] Since liquid handling and sample preparation are essential process steps for micro-total-analysis systems,[4–6] microfluidics are considered as a key technology within the promising sector of medical diagnostics.[7] Buzz features of microfluidic technologies are minimized consumption of sample and reagents, short time-to-result, and the amenability for process integration and parallelization. These market demands are addressed by so-called "lab-on-a-chip" systems which integrate basic analytical steps such as sample injection, separation, metering, mixing, reaction, and detection to perform complex diagnostic tasks on a credit card sized, microfluidic substrate.[8] Numerous approaches of innovative systems which involve proteomics,[9,10] immunoassays, *e.g.* HIV detection on-chip,[11] or DNA analysis,[12] account for the growing market demand.

A special type of these "lab-on-a-chip" systems are microstructured disks referred to as "lab-on-a-disk" platforms, which were investigated for the first time by Madou's group in 1998.[13,14] Common to these approaches is the exploitation of centrifugal forces to transport liquids. By setting the disk into spinning motion, the liquid passes sequentially arranged microfluidic structures,[15] performing processes like blood sedimentation,[16] metering, and mixing. In the final step, the sample reaches a detection chamber where the assay state is determined.[17,18]

Overall, lab-on-a-disk platforms possess a great potential for a comprehensive process integration of liquid handling and detection in miniaturized diagnostic assays[19–22] and—from the commercial point of view—numerous products have been launched to the market.[23–26]

For the widespread success of such lab-on-a-chip systems, the diffusion limited speed of mixing and reacting of liquids under strictly laminar conditions constitutes a major bottleneck. Among numerous technological solutions,[27–29] the induced chaotic advection by actuation of paramagnetic beads in an external field is of growing importance.[30,31] Most so far published setups exhibit a spatially fixed mixing chamber containing the magnetic beads. These beads are exposed to a time-varying magnetic field that is generated by a fixed array of current-oscillating electromagnets. Efficient mixing has been demonstrated in these devices; however, the need for miniaturized electromagnets severely increases the cost and complexity of these mixers.

Our novel lab-on-a-disk concept[32] simplifies the realization of magnetic-bead based mixing schemes. The magnetic beads are prefilled in a designated on-disk mixing chamber. A set of conventional permanent magnets resting in the lab-frame is specifically aligned in order to periodically divert the magnetic beads. Instead of applying a time-varying magnetic field, we rotate the chamber. This way, from the viewpoint of the magnetic beads, a time-oscillating magnetic force is generated by the spinning motion through a static magnetic field. Consequently, the beads are periodically deflected inbound and outbound which induces chaotic advection to the liquid phase by means of the Stokes drag. The beads therefore act as magneto-hydrodynamic transducers, drawing energy from the rotating motion which is converted by means of the magnetic field into an increase of the mixing entropy of the fluid.

Without magnetic beads, efficient mixing in the pure liquid is merely accomplished by inertially induced "twisting" currents during frequent alterations of the sense of rotation. Both strategies accelerate mixing to a similar extent. The mixing based on magnetic bead stirrers enables simple and efficient mixing if the centrifuge does not support a (rapid) change or even a frequent reversal of the sense of

rotation. On the other hand, the use of alternate spinning without magnetic beads avoids bead preparation and loading steps.

In both strategies, the coupling of the actuation delivered by the motion of the rotating drive into the hydrodynamic micromixing is very simple and robust, allowing a modular setup. The only active part of the setup, the rotating drive, is "macro", *i.e.* robust and reusable while the "micro"-parts are reduced to their functional essence, *i.e.* passive microstructures which can be fabricated in a very economic fashion, *e.g.* by industrial scale micromachining techniques such as hot-embossing or injection molding. Our mixing scheme can also be adopted for other stopped-flow circuitries which are compatible with centrifugal operation.[33]

In this paper, we first describe the actuation principle employed for our magnetic bead based mixing scheme. The laboratory setup is then introduced, the results obtained are presented, and a comprehensive analysis of the mixing performance for spinning at a constant frequency and spinning under frequent reversal of the sense of rotation is carried out.

2 Principle of mixing with magnetic beads

When exposed to an external magnetic field $\vec{B}$, paramagnetic particles, *i.e.* particles possessing a magnetic susceptibility χ ranging between 0 and 1, become attracted towards increasing $\vec{B}$. This phenomenon is based on the magnetization

$$\vec{M} = \frac{\chi}{(1+N_e)\chi}\frac{1}{m_0}\vec{B} \tag{1}$$

which is induced in the embedded magnetic dipoles by the magnetic flux density $\vec{B}$, with demagnetization-factor N_e and magnetic permeability μ_0.

A spherical magnetic particle (bead) of radius r_{bead} and volume

$$V_{bead} = \frac{4\pi}{3} r_{bead}^3 \tag{2}$$

experiences a force

$$\vec{F}_{mag} = \frac{V_{bead}}{m_0}\frac{\chi}{(1+N_e)\chi}\left(\vec{B}\nabla\right)\vec{B} \tag{3}$$

in a given magnetic field $\vec{B}$. The motion of a magnetic bead of mass m_{bead} and a velocity $\vec{u}$ in the rotating chamber is thus described by

$$m_{bead}\dot{\vec{u}} = \vec{F}_{mag} + \vec{F}_{centri} + \vec{F}_{Stokes} \tag{4}$$

taking into account the centrifugal force $\vec{F}_{centri}$ and the Stokes drag $\vec{F}_{Stokes}$. Substituting the above expressions yields

$$m_{bead}\dot{\vec{u}} = \frac{V_{bead}}{m_0}\frac{\chi}{(1+N_e)\chi}\left(\vec{B}\nabla\right)\vec{B} + V_{bead}(\rho_{bead}-\rho)(2\pi\nu)^2\vec{r} + 6\pi\eta r_{bead}\vec{u} \tag{5}$$

with the frequency of rotation ν, the viscosity η and the mass density ρ of the fluids to be mixed. For our calculations, the fluid is assumed to be at rest in the mixing chamber, *i.e.* in the frame of the rotating disk. To consider the dynamics of the system in more detail, the non-vanishing velocity field of the fluid phase due to the bead induced advection and inertial effects (as well as the Coriolis force) would have to be incorporated into eqn. (5).

3 Setup

Our novel setup comprises two distinguished modules, a disposable disk rotor (Fig. 1A) and an actuation and detection unit resting in the lab-frame. In the case of the magnetohydrodynamic mixing scheme, the designated mixing chamber as part of the disk is prefilled with magnetic beads.[34] They consist of Fe_3O_4 (50% vol) embedded in a polystyrene matrix exhibiting an experimentally determined magnetic susceptibility of $\chi = 0.95$. A saturation of the magnetization is achieved at an external flux density of $B_{sat} = 125$ mT. With a size of $r_{bead} = 68$ μm, the magnetic beads used here are significantly larger than comparable magnetic beads.[35–37] This is advantageous since, with increasing bead volume V_{bead}, the driving force $\vec{F}_{mag}$ (eqn. (3)) and the drag force in the surrounding liquid $\vec{F}_{Stokes}$ (eqn. (5)) grow to boost mixing.

The reusable actuation module comprises a rotation engine to spin the disk as well as a set of eight permanent magnets which are positioned closely above the microfluidic disk (Fig. 1A). Their spatial alignment alternatingly draws the magnetic beads inbound and outbound while passing the spatially periodic magnetic field.

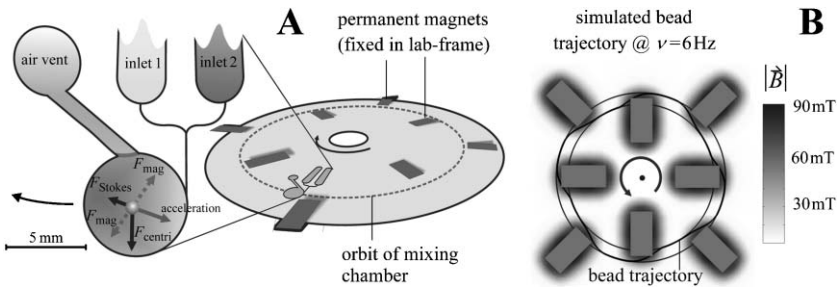

Fig. 1 (A) Concept of the rotating microfluidic disk and the forces acting on a paramagnetic bead: a set of permanent magnets is aligned in the lab-frame at radial positions which are positioned inbound and outbound relative to the mean orbit followed by the rotating mixing chamber (dashed circle). Thus, a confined magnetic bead experiences an alternating radial driving force $\vec{F}_{mag}$ which deflects the bead and induces advection *via* the viscous drag force $\vec{F}_{Stokes}$. The centrifugal force $\vec{F}_{centri}$ constantly points radially away from the center of rotation. (B) Computed trajectory of a magnetic bead as solution of the corresponding differential equation (eqn. (5)) for a spinning frequency $\nu = 6$ Hz. For $\nu = 6.5$ Hz, an equilibrium state (*i.e.*, optimum working point) is found.

The basic design of the microfluidic disk features two symmetric inlet reservoirs and an air vent which are individually connected by microchannels to the mixing chamber. Hydrophobic valves[38] are embedded in the inlet channels to avoid uncontrolled inflow. In our case, the retaining force of the hydrophobic valves is established by the interplay of a reduced channel cross-section with the hydrophobic Teflon patch on the surface. The round mixing chamber with a volume of 25 µl is subsequently connected to an outlet port. To prevent the beads from entering the outlet channel, its depth is more shallow than the diameter of the beads. Therefore, the channel acts as a geometrical barrier and retains the beads inside the mixing chamber.[39,40] All microfluidic disks are made of PMMA in the format of a compact disk (CD). They are structured by standard micromachining techniques.[41]

4 Simulation of bead trajectories

In order to promote efficient mixing *via* magnetic beads on a lab-on-a-disk, the beads ideally exhibit a high-amplitude deflection in different directions such that the bead trajectories cover the complete mixing chamber in time to rule out inhomogeneous mixing. Additionally, the deflection should be fast enough to transmit enough momentum *via* the Stokes drag onto the fluid. To meet these two requirements, we experimentally determined[42] the spatial distribution of the quantity $\left(\vec{B}\nabla\right)\vec{B}$ of the bar shaped permanent magnets.[43] $\left(\vec{B}\nabla\right)\vec{B}$ which is linearly correlated to the magnetic force $\vec{F}_{\mathrm{mag}}$ (eqn. (3)) exhibits a maximum value near the edges of the permanent magnets. Since a strong magnetic force is crucial for the deflection of the beads, it is straightforward to position the edges of the magnets right above the mixing chamber but slightly shifted inbound and outbound with respect to the mean orbit of the chamber.

The trajectory for one magnetic bead is simulated[44] by iteratively solving eqn. (5) for a given frequency of rotation ν and the determined spatial distribution of $\left(\vec{B}\nabla\right)\vec{B}$ (Fig. 1B). As further parameters, a demagnetization factor of $N_{\mathrm{e}} = 1/3$ for spheres and the geometry of the mixing chamber are applied.

We found an optimum frequency $\nu_{\mathrm{opt}} = 6.5$ Hz of stable periodic deflection where the counteracting forces balance on the average. For frequencies slightly below this optimum, the magnetic force prevails and the beads are trapped at the chamber wall in the vicinity of the magnets. For frequencies slightly above this optimum, the centrifugal force dominates and the bead does not return to its radial starting position. Thus, away from the optimum, the bead ensemble is, on average, either shifted to the inner or outer wall of the mixing chamber.

5 Experimental results

Mixing with magnetic beads

To conduct an experiment, the disk first has to be preloaded with a well-defined number of magnetic beads. Next, the two liquids are filled into the inlet reservoirs and the disk is set into spinning motion with a PC-controlled frequency curve $\nu(t)$.

The mixing process itself is initiated by an up-ramp until the burst-frequency of the hydrophobic inlet valves is exceeded. This way, magnetic beads which have entered the inlet channels are drawn outbound and therefore clogging of the inlets is prevented. Subsequently, the frequency of rotation is set to the designated mixing frequency ν. After mixing is completed, the frequency of rotation is elevated beyond the burst-frequency of the outlet valve to purge the mixing chamber.

Image acquisition was conducted with a microscope-mounted CCD-camera featuring an extremely short exposure time of 100 ns[45] to minimize smearing effects.[46] Each captured image is stored in an 8-bit grey-scale bitmap. The pixels which represent the beads are discarded to avoid artifacts in the subsequent evaluation. These bitmaps are transformed into an intensity histogram representing the full area of the mixing chamber and the standard deviation $\sigma(t)$ is evaluated (Fig. 2). Though the histogram does not follow a Gaussian distribution at the beginning of the mixing process, the standard deviation still constitutes an appropriate measure for the state of mixing. Along the mixing progress, the grey-scale distribution of the images becomes more uniform. Thus, the standard deviation $\sigma(t)$ exhibits a typical decay in time t, which is well approximated by an exponential curve $\sigma(t) \sim \exp(-t/\tau)$ where τ is referred to as the characteristic mixing time.

The mixing performance is mainly impacted by the frequency of rotation ν and the alignment of the magnets. Mixing can either be performed in constant spinning mode, *i.e.* ν = constant, as well as in alternate spinning ("shake") mode, *i.e.* $\nu = \nu(t)$ where the sense of rotation is reversed on a frequent basis. We first consider constant spinning mode.

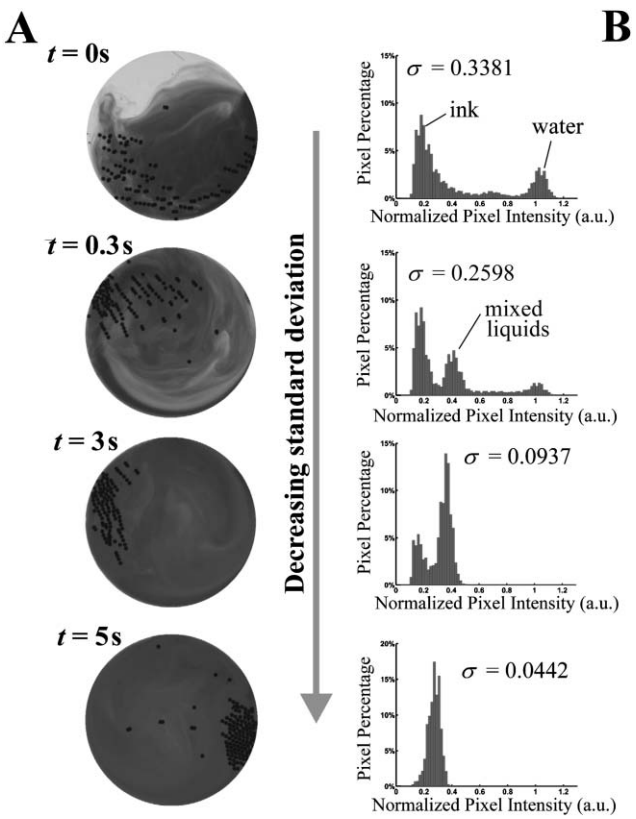

Fig. 2 Evaluation of the mixing progress, analyzed *via* acquired images (A) and 2D-histograms (B). As mixing proceeds, the distribution of pixel intensities shifts towards unity, *i.e.* the peak width in the histogram and thus the standard deviation $\sigma(t)$ diminishes.

Several series of experiments were carried out to optimize the mixing performance *via* the (constant) frequency ν. We experimentally identified a range of optimum frequencies ν between 5 Hz and 7 Hz. This experimentally determined frequency range is in good agreement to the computed solutions of the differential equation based on a simplified model (Fig. 1B).

For frequencies slightly above 7 Hz, the interplay of alternating inbound and outbound deflection of the beads by the magnets and the centrifugal force in constant spinning mode becomes unbalanced. As a consequence, the bead ensemble is shifted towards the outer wall of the mixing chamber. In this case, the mixing result is inhomogeneous across the mixing chamber, thus reducing the overall mixing performance.

For frequencies below this optimum frequency range, the filling process of the mixing chamber starts to become unpredictable in our current disk design, since the filling channels feature inherently embedded hydrophobic barriers exhibiting a burst frequency in the range of 5 Hz.

Mixing in alternate spinning mode

Even though mixing by periodically deflected magnetic beads inside the mixing chamber is already very efficient, the performance can further be improved by frequently changing the sense of rotation during mixing. These alternate spinning protocols are mainly characterized by the slope ν_{acc} of the ramp-up and ramp-down intervals as well as the maximum frequency ν_{max} of the frequency curve (Fig. 3A).

To understand the origin of the mixing effect, we consider the change of the spinning frequency for a given fluid element of a mass m_ω spaced at a radial distance r from the center of rotation (Fig. 4). Inertia tends to stabilize its angular velocity $\omega = 2\pi\nu$ and thus the angular momentum. According to the given geometry, a difference in the angular momentum

$$\Delta\Gamma_\omega = m_\omega\, \omega\, \Delta r \qquad (6)$$

arises from the difference in radial position Δr.

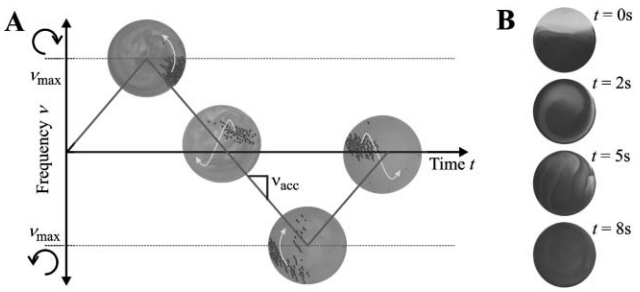

Fig. 3 Enhanced mixing by periodically alternating the sense of rotation: (A) Clockwise spinning shifts the beads towards the right wall, since the magnetic attraction tends to hold the beads and the moving chamber slips through underneath. Periodic alternation between fast and low spinning shifts the beads up- and downwards, respectively. As a result, zones in the mixing chamber which remain unaffected by the beads diminish. Optimum mixing is achieved for ν_{max} = 8 Hz and ν_{acc} = 32 Hz s^{-1}. (B) Without magnetic beads, the frequent reversal of the sense of rotation still impacts on the inertia of the liquid to induce advective currents (mixing).

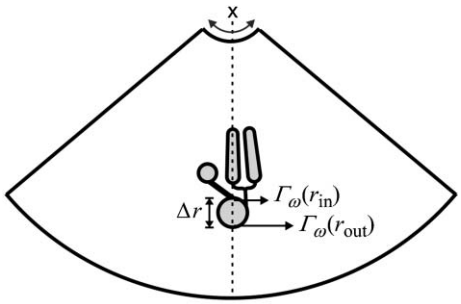

Fig. 4 The radial extension Δr of the mixing chamber causes a gradient in the angular momentum $\Delta\Gamma_\omega$ according to eqn. (6). In consequence, a shear-driven advective current arises within the liquid phase upon acceleration and deceleration.

In our disk geometry, the cylindrical mixing chamber features a diameter of Δr = 6 mm at an inner distance to the center of r_{in} = 39 mm, which, according to eqn. (6), corresponds to a radial difference of the angular momentum of $\Delta\Gamma_\omega > 15\%$. This difference in the angular momentum translates into a shear force which drives an advective current within the fluid upon acceleration and deceleration. Mixing is promoted by a twisting pattern of the two fluids shown in Fig. 3B compared to mere deflection of the magnetic beads in constant spinning mode where the angular momentum Γ_ω does not change in time to eliminate these inertially induced shear forces.

The alternate spinning mode also induces an azimuthal (lateral) deflection of the bead ensemble within the mixing chamber to further extend the overall area of bead induced mixing. Fig. 3A displays the experimentally observed trajectories of the bead ensemble deflected in alternate spinning mode at different angular positions over five cycles.

For an experimental evaluation, we compare the observed characteristic mixing time τ (Fig. 5) for the different modes of mixing for a 25 µl volume. As a reference, mere diffusive mixing lasts 7 min (Fig. 5, squares). The hydrodynamic twisting patterns of the pure liquid (without beads) in alternate spinning drastically reduces the mixing time down to 3.0 s (Fig. 5, triangles). An even better performance is achieved by bead-based mixing in constant spinning mode, reaching a mixing time of 1.3 s, only (Fig. 5, diamonds). The best mixing performance (0.5 s) is achieved by combining the two strategies, *i.e.* magnetic-bead based mixing in alternate spinning mode (Fig. 5, circles).

6 Summary and conclusion

We have presented two novel concepts for mixing of liquids for centrifugal lab-on-a-disk platforms. The mechanism of mixing is rooted in two fundamental schemes of inducing advection: the magneto-hydrodynamic interaction of magnetic beads with a static, external magnetic field and the inertia of the liquids upon acceleration and deceleration in alternate spinning "shake" mode.

In the first mode, magnetic beads are filled in a disk-based mixing chamber. The disk is exposed to a magnetic field created by a set of permanent magnets resting in the lab-frame.

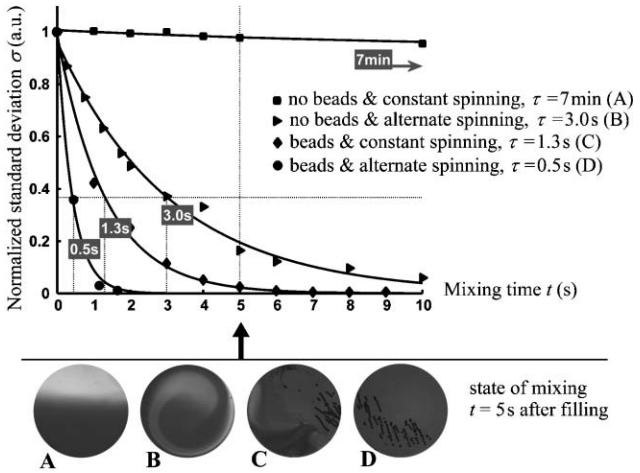

Fig. 5 Decrease of the standard deviation $\sigma(t)$ as mixing proceeds: As a benchmark, a characteristic mixing time τ is defined as the 1/*e*-decay of $\sigma(t)$. Compared to mere diffusion (A) with τ = 7 min, the alternate spinning ("shake-mode") mode without beads (B) with τ = 3.0 s and the bead-based mixing in constant spinning mode (C) with τ = 1.3 s drastically speeds up mixing. This improvement is even outperformed by bead-based magneto-hydrodynamic mixing in alternate spinning mode (D) which accelerates mixing to τ = 0.5 s, *i.e.* by three orders of magnitude.

Setting the disk into spinning motion, the beads follow the orbit of the chamber to experience a time-oscillating magnetic field. The suspended beads are periodically deflected within the chamber to induce advection in the liquid by means of the Stokes drag.

In the second "shake" mode, periodic changes of the sense of rotation transfer a gradient of angular momentum into arising advective currents within the fluid upon acceleration and deceleration. Combining both schemes, mixing of a 25 µl volume is accomplished within less than 1 s, *i.e.* an acceleration by three orders of magnitude compared to mere diffusion.

Our concept displays several advantages compared to other active micromixing schemes: First, it is based on a simple and modular setup which avoids 3D-micromachining, moving microparts, on-chip actuators and current controlled micro-coils to invoke deflection of magnetic beads in a chamber at rest. Additionally, rather low spinning frequencies in the range of 5–10 Hz are required which is below typical burst frequencies of hydrophobic valves. The concept can thus readily be integrated in common centrifugal microfluidic platforms. Finally, the concept can be applied to a broad range of volumes between the microliter and the milliliter scale.

Acknowledgements

The authors are grateful to the support by the German federal state of Baden-Wuerttemberg (grant number 24-720.431-1-7/2) and good cooperation with HSG-IMIT[47] and Jobst Technologies.[42]

M. Grumann, A. Geipel, L. Riegger, R. Zengerle and J. Ducrée
IMTEK—University of Freiburg, Laboratory for MEMS Applications, Georges-Koehler-Allee 106, D-79110 Freiburg, Germany.
E-mail: grumann@imtek.de www.imtek.delanwendungen

References

1 D. Harrison, C. Wang, P. Thibeault, F. Ouchen and S. Cheng, The decade search for the killer ap in µ-TAS, *Proceedings of the µTAS 2000 Symposium*, ed. W. Olthuis, A. van den Berg and P. Bergveld, Kluwer Academic Publisher, 2000, pp. 195–204.
2 *FlowMap—Microfluidics roadmap for the life sciences*, ed. J. Ducrée and R. Zengerle, Books on Demand GmbH, Norderstedt, Germany, 2004, http://www.microfluidics-roadmap.com, ISBN 3-8334-0744-1.
3 http://www.myFluidix.com—Free Online Resources in Microfluidics, 2003.
4 D. Reyes, D. Iossifidis, P. Auroux and A. Manz, Micro total analysis systems. 1. Introduction, theory, and technology, *Anal. Chem.*, 2002, **74**, 12, 2623–2636.
5 P. Auroux, D. Reyes, D. Iossifidis and A. Manz, Micro total analysis systems. 2. Analytical standard operations and applications, *Anal. Chem.*, 2002, **74**, 12, 2637–2652.
6 *Micro Total Analysis Systems*, ed. A. van den Berg and E. Oosterbroek, Elsevier Science, Amsterdam, NL, 2003.
7 T. Schulte, R. Bardell and B. Weigl, Microfluidic technologies in clinical diagnostics, *Clin. Chim. Acta*, 2002, **321**, 1–2, 1–10.
8 D. Figeys and D. Pinto, Lab-on-a-chip: A revolution in biological and medical sciences, *Anal. Chem.*, 2000, **72**, 9, 330–335A.
9 L. Bousse, S. Mouradian, A. Minalla, H. Yee, K. Williams and R. Dubrow, Protein sizing on a microchip, *Anal. Chem.*, 2001, **73**, 6, 1207–1212.
10 D. Figeys and D. Pinto, Proteomics on a chip: Promising developments, *Electrophoresis*, 2001, **22**, 2, 208–216.
11 S. Sia, V. Linder, B. Parviz, A. Siegel and G. Whitesides, An integrated approach to a portable and low-cost immunoassay for resource-poor settings, *Angew. Chem. Int. Ed.*, 2004, **43**, 498–502.
12 J. Khandurina, T. McKnight, S. Jacobson, L. Waters, R. Foote and J. Ramsey, Integrated system for rapid PCR-based DNA analysis in microfluidic devices, *Anal. Chem.*, 2000, **72**, 13, 2995–3000.
13 M. Madou and G. Kellogg, LabCD: A centrifuge-based microfluidic platform for diagnostics, *Proc. SPIE*, 1998, **3259**, 80–93.
14 M. Madou, Y. Lu, S. Lai, J. Lee and S. Daunert, *A Centrifugal Microfluidic Platform: A Comparison, Proceedings of the µTAS 2000 conference*, ed. A. van den Berg and P. Bergveld, Kluwer Academic Publisher, 2000, pp. 565–570.
15 G. Ekstrand, C. Holmquist, A. E. Örleforn, B. Hellmann, A. Larsson and P. Andersson, *Microfluidics in a rotating CD, Proceedings of the µTAS 2000 conference*, ed. A. van den Berg and P. Bergveld, Kluwer Academic Publisher, 2000, pp. 311–314.
16 T. Brenner, S. Haeberle, R. Zengerle and J. Ducrée, *Continuous Centrifugal Separation of Whole Blood on a Disk, Proceedings of the µTAS 2004 conference*, ed. T. Laurell, J. Nilsson, K. Jensen, D. J. Harrison and J. P. Kutter, Royal Society of Chemistry, 2004, pp. 566–568.
17 D. Walt, Bead-based Fiber-Optic Arrays, *Science*, 2000, **287**, 5452, 451–452.
18 M. Grumann, I. Moser, J. Steigert, L. Riegger, A. Geipel, C. Kohn, G. Urban, R. Zengerle and J. Ducrée, *Optical Beam Guidance in Monolithic Polymer Chips for Miniaturized Colorimetric Assays, Proc. 18th IEEE conference*, MEMS 2005, Miami, USA, pp. 108–111, 2005.
19 C. Schembri, T. Burd, A. Kopf-Sill, L. Shea and B. Braynin, Centrifugation and Capillarity integrated into a multiple analyte whole blood analyser, *J. Autom. Chem.*, 1995, **17**, 3, 99–104.
20 I. Badr, R. Johnson, M. Madou and L. Bachas, Fluorescent Ion-Selective Optode Membranes Incorporated onto a Centrifugal Microfluidics Platform, *Anal. Chem.*, 2002, **74**, 5569–5575.
21 S. Lai, S. Wang, J. Luo, L. Lee, S. Yang and M. Madou, Design of a Compact Disk-like Microfluidic Platform for Enzyme-Linked Immunosorbent Assay, *Anal. Chem.*, 2004, **76**, 1832–1837.
22 L. Puckett, E. Dikici, S. Lai, M. Madou, L. Bachas and S. Daunert, Investigations into the Applicability of the Centrifugal Microfluidics Platform for the Development of Protein–Ligand Binding Assays Incorporating Enhanced Green Fluorescent Protein as a Fluorescent Reporter, *Anal. Chem.*, 2004, **76**, 7263–7268.
23 LabCD™, Tecan Group Ltd., Switzerland, http://www.tecan.com.

24 Gyrolab Bioaffy CD, Gyros AB, Sweden (formerly Pharmacia Inc., USA), http://www.gyros.com.
25 Pelikan Sun™ of Pelikan Technologies Inc., USA, http://www.pelikantechnologies.com.
26 Piccolo, Abaxis Inc., USA, http://www.abaxis.com.
27 D. Kim, S. Lee, T. Kwon and S. Lee, *Barrier embedded chaotic micromixer, Proceedings of MEMS-conference*, IEEE Trans., pp. 339–342, 2003.
28 J. Ducrée, T. Brenner, T. Glatzel and R. Zengerle, *A Coriolis-based split-and-recombine laminator for ultrafast mixing on rotating disks, Proceedings of μTAS 2003 conference*, ed. M. A. Northrup, K. F. Jensen, and D. J. Harrison, MESA Monographs, pp. 903–906, 2003.
29 T. Brenner, T. Glatzel, R. Zengerle and J. Ducrée, Frequency dependent transversal flow control in centrifugal microfluidics, *Lab Chip*, 2005, **5**, 146–150.
30 A. Rida, T. Lehnert and M. Gijs, *Micro mixer using magnetic beads, Proceedings of μTAS 2003 conference*, ed., M. A. Northrup, K. F. Jensen and D. J. Harrison, MESA Monographs, 2003, pp. 579–581.
31 R. Rong, J. Choi and C. Ahn, *A novel magnetic chaotic mixer for in-flow mixing of magnetic beads, Proceedings of μTAS 2003 conference*, ed. M. A. Northrup, K. F. Jensen, and D. J. Harrison, MESA Monographs, 2003, pp. 335–338.
32 J. Ducrée, T. Brenner, M. Grumann, W. Bessler, M. Stelzle, S. Messner, T. Nann, J. Ruehe, I. Moser and R. Zengerle, *Bio-Disk—A centrifugal platform for integrated point-of-care diagnostics on whole blood*—http://www.bio-disk.com.
33 G. Thorsén, G. Ekstrand, U. Sedlitz, S. Wallenborg and P. Andersson, *Integrated Microfluidics for Parallel Processing of Proteins in a CD Microlaboratory, Proceedings of μTAS 2003 conference*, ed. M. A. Northrup, K. F. Jensen and D. J. Harrison, MESA Monographs, 2003, pp. 457–460,.
34 Microparticles GmbH, Berlin, Germany, http://www.microparticles.de.
35 Promega Corp. USA, $r_{bead} < 10$ μm, http://www.promega.com.
36 Dynabeads^{R} with $r_{bead} < 300$ nm, Dynal Biotech, Norway, http://www.dynalbiotech.com.
37 Sphero™ with $r_{bead} < 10$ μm, Spherotech Inc., USA, http://www.spherotech.com.
38 M. Madou, L. Lee, S. Daunert, S. Lai and C. Shih, Design and Fabrication of CD-like Microfluidic Platforms for Diagnostics: Microfluidic Functions, Biomedical Microdevices 3:3, pp. 245–254, 2001.
39 M. Grumann, P. Schippers, M. Dobmeier, S. Haeberle, A. Geipel, T. Brenner, C. Kuhn, M. Fritsche, R. Zengerle and J. Ducrée, Formation of hexagonal monolayers by flow of bead suspensions into flat microchambers, Proceedings of IMECE (ASME), 2003–41427, 2003.
40 M. Grumann, M. Dobmeier, P. Schippers, T. Brenner, R. Zengerle and J. Ducrée, The Model of Porous Media—Complete Description for aggregation of bead-monolayers in flat microfluidic chambers, *Lab Chip*, 2004, **4**, 209–213.
41 Jobst Technologies, Germany, http://www.jobst-technologies.com, 2004.
42 Teslameter 6010, F. W. Bell, Cunz GmbH, Germany, http://www.cunz.de, 2004.
43 NdFeB-magnets, order-no. J54-307, Edmund Industrie Optik GmbH, Germany, http://www.edmundoptics.com, 2003.
44 Matlab 6.5.0, The Mathworks Inc. USA, http://www.mathworks.com, 2003.
45 Sensicam fast shutter 370KF, PCO Computer Optics GmbH, D-93309 Kehlheim, Germany, http://www.pco.de.
46 M. Grumann, T. Brenner, C. Beer, R. Zengerle and J. Ducrée, Visualization of flow patterning in high speed centrifugal microfluidics, *Rev. Sci. Instrum.*, 2005, **76**, 2, 025101.
47 HSG-IMIT, Institute for Micromachining and Information Technology, Germany, http://www.hsg-imit.de.